Journal of Magnetic Resonance 321 (2020) 106856

Contents lists available at ScienceDirect

Journal of Magnetic Resonance

journal homepage: www.elsevier.com/locate/jmr

Fast remote correlation experiments for ^{1}H homonuclear decoupling in solids

Pinelopi Moutzouri, Bruno Simões de Almeida, Lyndon Emsley *

Institut des Sciences et Ingéniere Chimiques, École Polytechnique Fédérale de Lausanne (EPFL), CH-1015 Lausanne, Switzerland

ARTICLE INFO

Article history:
Received 9 September 2020
Revised 19 October 2020
Accepted 20 October 2020
Available online 22 October 2020

Keywords:
Solid-state NMR
^{1}H resolution
Magic angle spinning
Anti-z-COSY
TOP

ABSTRACT

In ^{1}H MAS spectra, the residual homogeneous broadening under MAS is due to a combination of higher-order shifts and splittings. We have recently shown how the two-dimensional anti-z-COSY experiment can be used for the removal of the splittings. However, this requires spectra with high resolution in the indirect dimension (t_1), leading to experiment times of hours. Here, we show how anti-z-COSY can be adapted to be combined with the two-dimensional one pulse (TOP) transformation which leads to significantly reduced experimental time while retaining the line narrowing effect. The experiment is demonstrated on a powdered sample of L-histidine monohydrochloride monohydrate, where the new TAZ-COSY sequence at 100 kHz MAS, yields between a factor 1.6 and 2.3 increase in resolution compared with the equivalent one-pulse experiment, in just 20 min. The same methodology is also adapted for the acquisition of liquid state ^{1}H homodecoupled data, and an example is given for testosterone.

1. Introduction

Spectral resolution in ^{1}H spectra of solids is often hampered by the presence of interactions that lead to homogeneous or inhomogeneous broadening of the NMR signals [1]. Among those, ^{1}H homonuclear dipolar interactions, which in organic solids can usually be of the order of a few kHz, are quite strong and usually contribute to a large extent to the spectral linewidths. Magic angle spinning (MAS) [2] averages out homonuclear dipolar interactions yielding spectra with significantly improved resolution. Faster spinning speeds produce narrower proton linewidths. However, today, at the fastest rates available (between 100 and 150 kHz MAS) [3], linewidths remain orders of magnitude broader that those encountered in liquid samples. At more modest spinning rates, pulse sequences designed to remove homonuclear dipolar couplings [4] can be combined with MAS to produce extra narrowing [5]. At 100 kHz the linewidths obtained with MAS alone are about the same as the best results from state-of-the-art CRAMPS at lower MAS rates, and so far CRAMPS schemes have yielded no significant improvement for MAS rates above 100 kHz.

Recently we have introduced an alternate approach to achieving ^{1}H homonuclear decoupling at 100 kHz MAS that does not rely on multiple-pulse averaging sequences to remove the homonuclear dipolar Hamiltonian [6]. The anti-*z*-COSY experiment [7] exploits a simple 2D scheme that yields correlations between remote transitions of the coupling partners, and a 45° projection taken across the diagonal peaks of a phase-sensitive 2D spectrum removes the residual splittings due to homonuclear dipolar interactions. The selection of the remote transitions is done by the use of small flip angle two-pulse block. The approach typically yields up to a factor of two improvement in resolution compared with conventional spectra acquired at the same MAS rate. At fast MAS rates this approach yields the highest resolution ^{1}H MAS spectra available today [6].

However, one main drawback of this approach is the need to record a two-dimensional spectrum with high resolution in both dimensions, which more often than not can be quite time-consuming. Typically, hundreds of points are required in t_1, leading to acquisition times of hours. Here, we show how a modification of the pulse sequence and the acquisition scheme can offer identical results in terms of spectral resolution but in a few minutes. We combine the anti-*z*-COSY experiment with an affine transformation [8]. This enables the remapping of the data to allow narrow spectral widths to be acquired in the indirect dimension. This approach speeds up the acquisition times of the anti-*z*-COSY experiment by a factor of 15 or more, while maintaining here peaks up to a factor of 2.3 narrower than in the conventional one-pulse one-dimensional experiment at the same MAS rate.

* Corresponding author.
E-mail address: lyndon.emsley@epfl.ch (L. Emsley).

https://doi.org/10.1016/j.jmr.2020.106856
1090-7807/

2. Methods

2.1. Modification of the anti-z-COSY pulse sequence

As described in detail previously [6–7], the anti-*z*-COSY pulse sequence consists of an initial excitation 90° pulse followed by an evolution period t_1 and a mixing element of the form, 180°+β° − τ_z − β°, where β denotes a small flip angle, as shown in Fig. 1a. The sequence of Fig. 1b is modified in order to maintain the criteria needed for the application of the affine transformation and to allow whole echo acquisition in t_1 [9]. The affine transformation which consists in a series of shearing transformations will allow under-sampled spectra in t_1 to inherit the spectral properties in t_2 after transformation. This was first used in NMR in the context of Two-dimensional One Pulse (TOP) experiments [10]. In the experiment of Fig. 1b, the 180° pulse and the low flip angle *z*-filter, β° − τ_z − β°, are placed in the middle of the evolution period, t_1. At this position this element allows the pure chemical shift evolution to be sampled in the indirect dimension independently of the effects of homonuclear coupling. In analogy with approaches to pure shift spectroscopy in solution NMR [11], the small flip angle building block together with the 180° pulse thus only yields correlations between remote transitions since any splittings caused by homonuclear coupling to other spins are suppressed through the inversion of the spin state of their coupling partners by the 180° pulse. As illustrated in Fig. 2a, the time domain of this experiment consists in pure chemical shifts along t_1 and the sum of shifts and residual couplings in t_2. Compared to the anti-*z*-COSY experiment, the shape of the diagonal peaks is no longer perpendicular to the diagonal of the spectrum but is now parallel to the direct dimension.

A further modification lies in the 2D scheme used for the acquisition of the two-dimensional absorptive phase-sensitive spectrum. For the parent anti-*z*-COSY experiment a States-TPPI hypercomplex acquisition [12] is typically used, for which two different data sets with quadrature phases for the initial excitation pulse are acquired. In the TAZ-COSY sequence, pure absorption mode lineshapes can be achieved simply by collecting the first half of the indirect increments with the sequence shown in Fig. 1b, that records a positive sense of evolution for the chemical shift interaction, and the second half with the sequence shown in Fig. 1c, that records respectively a negative sense of evolution. This leads to whole echo acquisition in t_1 [9], and upon 2D Fourier transformation, absorption mode data are acquired without the necessity of an additional *z*-filter at the end of the sequence scheme.

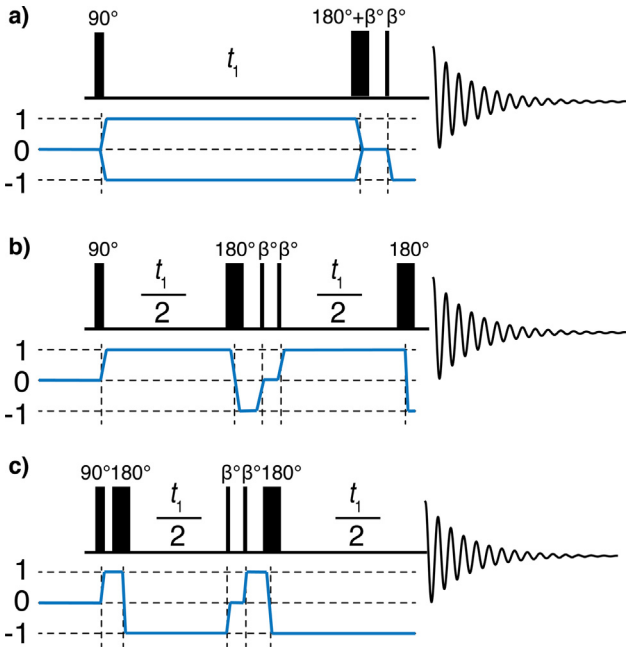

Fig. 1. (a) Anti-*z*-COSY pulse sequence and coherence pathway. (b, c) TAZ-COSY pulse sequence and coherence-transfer pathways for the acquisition of a) the echo and b) the anti-echo part of the signal. Here, β indicates a low-flip-angle pulse.

2.2. Data processing: Shearing and symmetrization

This data structure allows the affine transformation to be applied in a similar way as in the 2D TOP-PASS experiment described by Davis et al. [8b], since the dataset as acquired separates the chemical shift evolution, which evolves along t_1 from the evolution due to homonuclear couplings, which proceeds along the negative diagonal, $\varepsilon = -t_1/t_2$. This is illustrated in Fig. 2a. The affine transformation remaps the data such that the two interactions, chemical shift and homonuclear couplings, lie along the horizontal and vertical axis respectively while simultaneously inheriting the sampling properties of the axis onto which they are transformed [8b]. Through this approach, it is possible to record data that are heavily undersampled in the indirect dimension.

This allows us to reduce the spectral width and number of increments in the indirect dimension, since it will only contain the residual dipolar broadening in the final spectrum. As a result, the peaks will be folded along t_1 in the raw spectrum, and the affine transformation here consists in applying two sequential active shearing transformations as shown in Fig. 2b–e:

$$\begin{bmatrix} t_1' \\ t_2' \end{bmatrix} = \underbrace{\begin{bmatrix} 1 & 0 \\ -1 & 1 \end{bmatrix}}_{\kappa_2} \underbrace{\begin{bmatrix} 1 & +1 \\ 0 & 1 \end{bmatrix}}_{\kappa_1} \begin{bmatrix} t_1 \\ t_2 \end{bmatrix}$$

The scheme presented allows us to reduce the experimental time here by a factor of 16.5. Note that a similar shearing based approach was used in the initial anti-*z*-COSY article [7a].

As shown in Fig. 2b, when the spectral width of the indirect dimension is reduced, the diagonal folds into parallel sections, which remain tilted at a 45° with respect to both of the axes of the 2D plot. The diagonal peak shapes all remain parallel to the direct axis. In the frequency domain the first shear, which is parallel to F1 and has a shearing factor of −1, leads to the spectrum shown in Fig. 2c. Any sections that ended up outside the original spectral window during the first shearing process have been wrapped back inside. Finally, in Fig. 2d, the second shear, which is parallel to the F2 dimension and has a shearing factor of +1, aligns the multiplets to be parallel to F1. At this point a sum projection about the cross section F1 = 0 can be taken and the extracted 1D spectrum is free from any broadening due to homonuclear couplings.

Folding of the spectrum does not affect the diagonal peaks in the final spectrum, since in the 2D double-sheared spectrum they will be symmetrically distributed about the cross section and centered at F1 = 0. However, as shown in Fig. 2d, this will not be the case for the cross peaks, or anything else that is not a diagonal peak. (Weak cross peaks are sometimes observed in anti-z-COSY spectra of solids, as discussed in reference [6]). In most cases, they will be folded/wrapped in positions that are no longer symmetric with respect to their partners. We can therefore exploit this characteristic to remove them from the final 2D spectrum by applying a symmetrization procedure perpendicular to ω_2. This will remove all the cross peaks, unless by chance they have folded in symmetrical positions. In cases where their final position in the doubly-

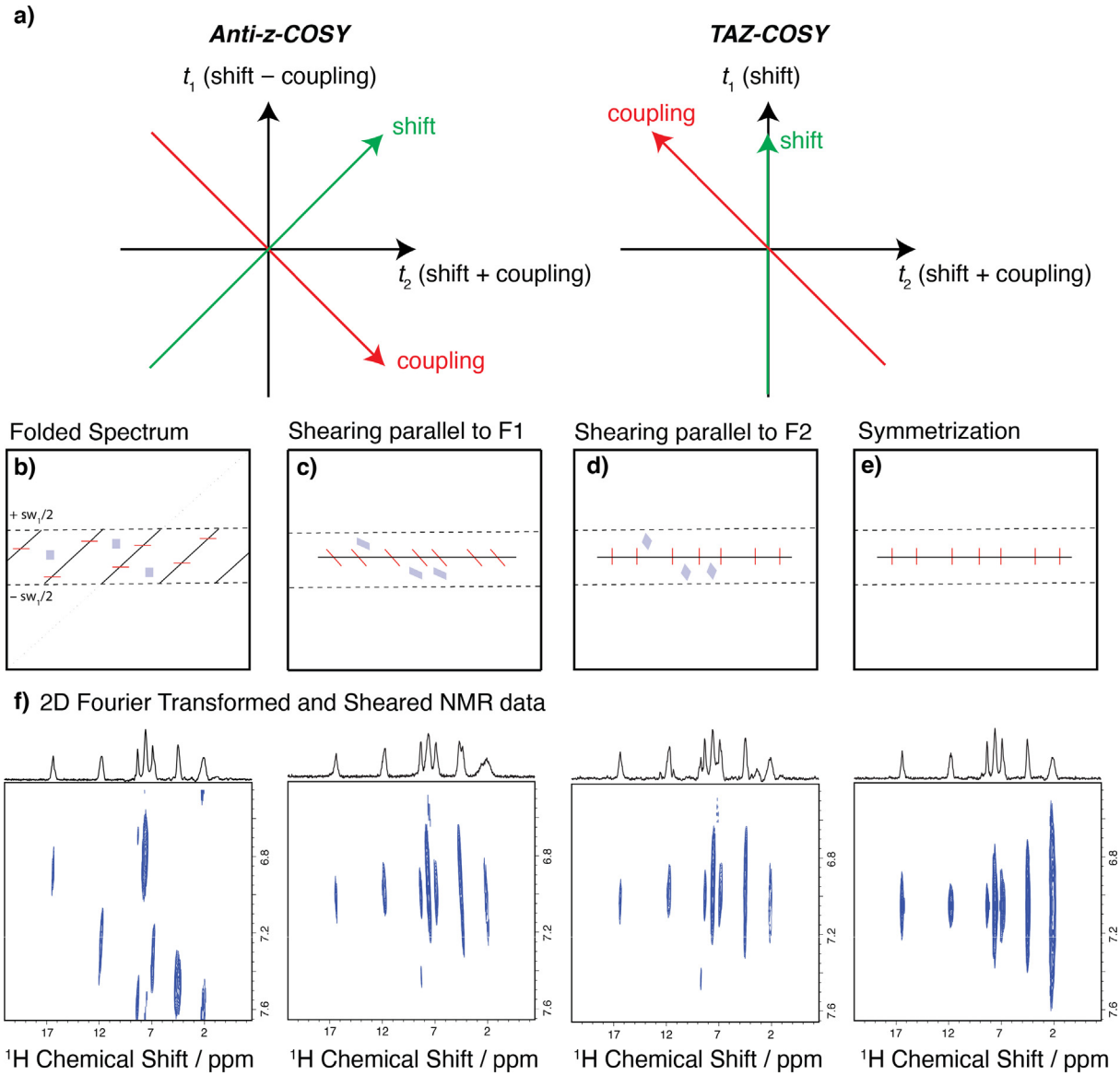

Fig. 2. (a) Representation of the time-domain data structure for an anti-*z*-COSY and a TAZ-COSY experiment. (b) Schematic representation of a folded spectrum between the $+sw_1/2$ and $-sw_1/2$ limits, where diagonal peaks are represented as solid red lines and cross peaks as blue boxes. (c) First shear parallel to F1 with a shearing rate of -1. (d) Second shear parallel to F2 with a shearing rate of +1. (e) Symmetrization of the spectrum shown in d). (f) Exemplification of the shearing process and of the symmetrization with NMR data acquired with the sequences shown in Fig. 1b and c for L-Histidine monohydrochloride monohydrate. The processing scripts used here are provided in SI. (For interpretation of the references to colour in this figure legend, the reader is referred to the web version of this article.)

sheared spectrum coincides with a diagonal peak, symmetrization can perturb the intensity of the diagonal peak.

(Note that the approach described above can be also applied for the acquisition of homonuclear *J* decoupled proton spectra in the liquid state. A sequence and an example can be found in the Supplementary Information of this manuscript.)

3. Results and discussion

Fig. 3 shows the linewidths achieved with the pulse sequences of Fig. 1b and c and the processing described in Fig. 2 for a powdered sample of L-Histidine monohydrochloride monohydrate, acquired at 298 K and with a 100 kHz MAS rate. The pulse flip angles β tested range from 90° to 5°, and the bar chart of Fig. 3f clearly shows the expected dependence of the ^{1}H homonuclear decoupling efficiency on the β angle. At β = 5° we measured linewidths of 269, 164, 174, 189, 163, and 214 Hz for protons H1, H5, H6, H7, H8, and H9 respectively as compared to 364, 308, 211, 330, 223, and 461 Hz in the TAZ-COSY experiment acquired with β = 90° and to 563, 380, 346, 408, 376, and 682 Hz in the 1D spectrum acquired with the conventional spin-echo experiment. We note that in this sample the water molecule is thought to be static, and the two protons are crystallographically inequivalent and will therefore be strongly coupled, and lead to a characteristic splitting which is removed by the TAZ-COSY experiment.

The spectra were acquired with a highly reduced spectral window in F1, specifically a width of 2000 Hz was used and only 16 increments were acquired in the indirect dimension. As a result, the amount of experimental time needed to acquire the spectrum was reduced by a factor 8.25 compared to a conventional full anti-z-COSY spectrum. The span of the integral projection was taken according to the width of the narrowest peak in ω_1.

In Fig. 4 the spectra measured with the new TAZ-COSY sequence and the previously reported anti-*z*-COSY sequence (with a full

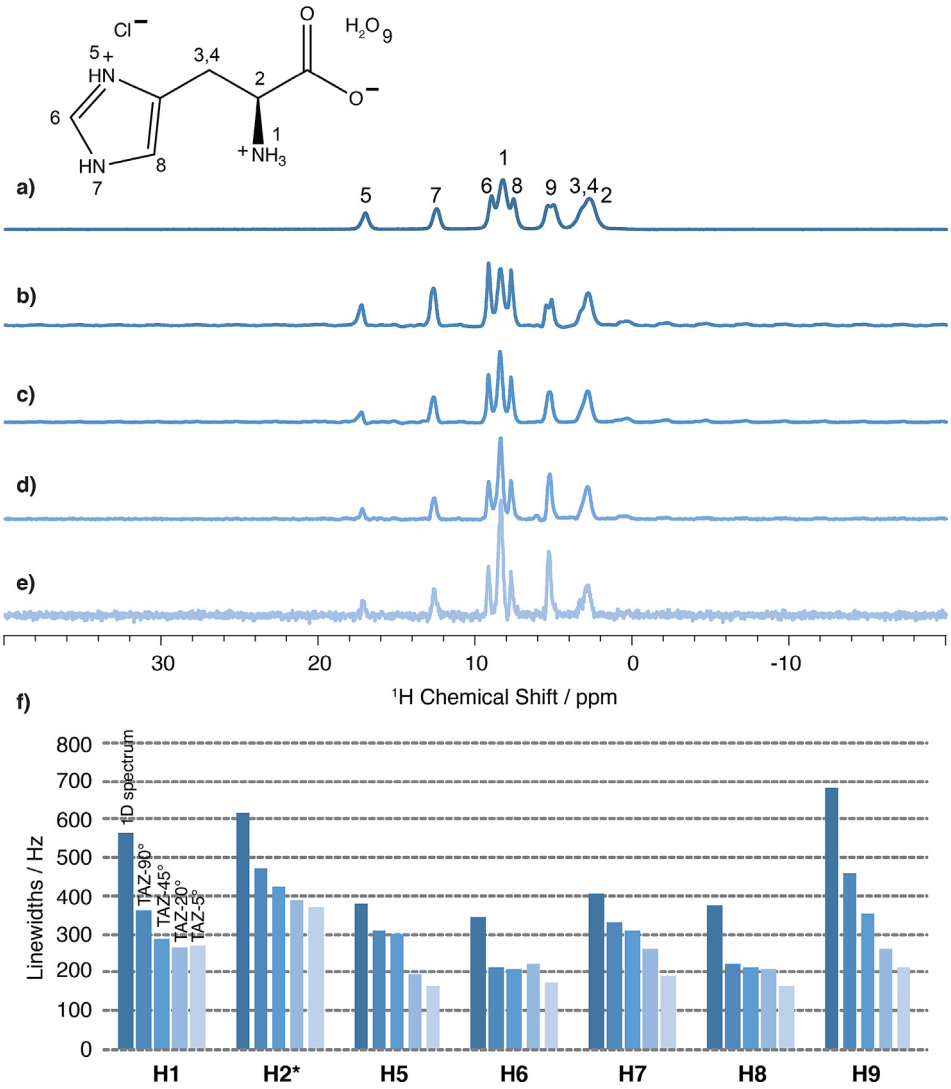

Fig. 3. (a) Echo-detected 100 kHz MAS spectrum of powdered microcrystalline L-Histidine monohydrochloride monohydrate. (b–e) Spectra obtained from integral projections of the TAZ-COSY spectrum acquired at 100 kHz MAS, with β angle of 90°, 45°, 20°, and 5°. (f) Measured linewidths of the spin-echo experiment and of the TAZ-COSY projections as a function of β. The asterisk on H2 denotes overlapping resonance peaks. See SI for full details.

spectral width in the indirect dimension) are compared. The comparison was performed for two different MAS spinning rates, at 50 and at 100 kHz. The 50 kHz MAS data were recorded with an indirect spectral width of 16.6 kHz, with 128 increments, 16 scans and a recycle delay of 5 s for the unfolded full anti-*z*-COSY spectrum, and with an indirect spectral width of 1.0 kHz, 16 increments, 16 scans and a recycle delay of 5 s for the TAZ-COSY spectrum. The 100 kHz MAS data were recorded with an indirect spectral width of 16.6 kHz, 122 increments, 32 scans and a recycle delay of 5 s for the unfolded full anti-*z*-COSY spectrum and with an indirect spectral width of 1.0 kHz, 8 increments, 32 scans and a recycle delay of 5 s for the TAZ-COSY spectrum.

In both cases, the spectra extracted from the data acquired with either a full or a folded indirect spectral width look essentially identical. The resolution enhancement obtained from anti-z-COSY is fully preserved in the TAZ-COSY spectrum. (Table S4 provides a numerical comparison of the measured linewidths for each peak in the spectrum.) The key difference lies in the experimental time. With the TAZ-COSY we can acquire a high-resolution spectrum in only twenty minutes, which is 16.5 times faster than the full anti-z-COSY which took nearly 6 h.

We note that the water and aliphatic resonances in Fig. 4 e and f show minor lineshape distortions that we have previously seen in the anti-*z*-COSY experiments and which we attribute to strong coupling effects [6].

Practical aspects concerning the set-up of a TAZ-COSY experiment include the selection of the correct indirect spectral width and the correct number of points to be recorded in the indirect dimension. The spectral width in t_1 should be wide enough in order to fit the untruncated residual dipolar broadening. In most cases a spectral width between 500 and 2000 Hz should suffice. The number of increments should be sufficient to yield a $t_{1\max}$ that avoids truncation of the residual dipolar broadening. Depending on the choice of indirect spectral width, a number of t_1 increments between 4 and 16 should be appropriate. Finally, it should be noted that a reduced signal to noise ratio is obtained in the rapid TAZ-COSY projections, as compared to the full anti-*z*-COSY projections, which is simply due to the reduced time-averaging. The signal to noise ratio per unit time should be equivalent (more details can be found in Table S5).

4. Conclusions

In summary, we have introduced a modified anti-*z*-COSY sequence that is compatible with the TOP transform and whole echo acquisition and which here results in a factor of 16.5

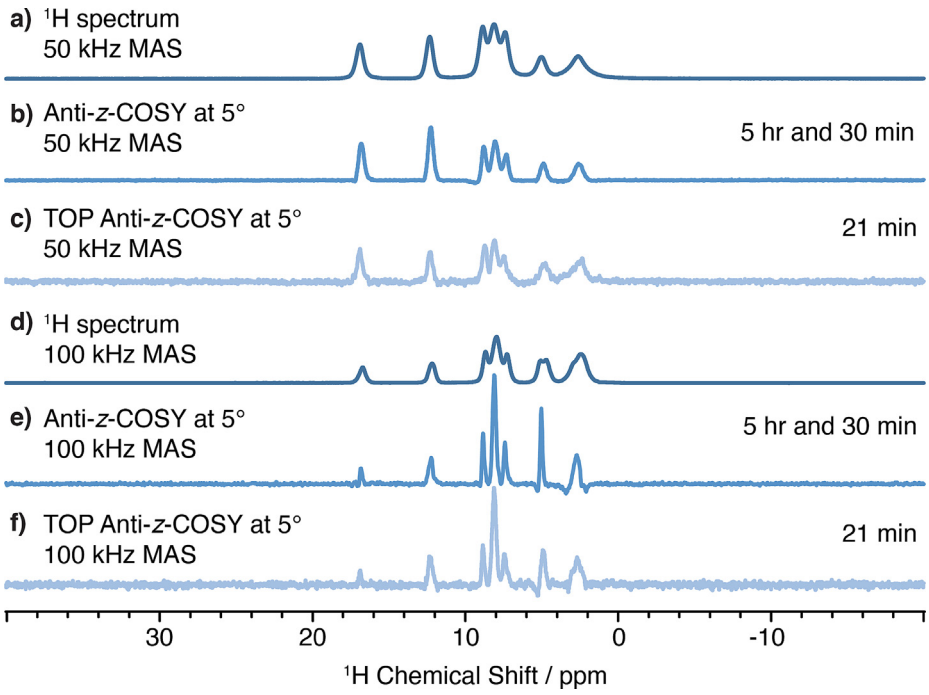

Fig. 4. (a) and (d) echo-detected 50 and 100 kHz MAS spectra of powdered microcrystalline L-Histidine monohydrochloride monohydrate. (b) and (e) 1D spectra obtained as integral projections of an anti-*z*-COSY spectrum acquired with a full spectral with in the indirect dimension and with a β of 5°. (c) and (f) 1D spectra obtained as integral projections from a TAZ-COSY spectrum acquired with an indirect spectral width of 1000 Hz and with a β of 5°. See SI for full details.

reduction in the experimental time required to obtain ^{1}H remote correlation spectra in solids. We used the resulting TAZ-COSY sequence to obtain spectra from powdered microcrystalline L-Histidine monohydrochloride monohydrate at both 50 and 100 kHz MAS rates, where we confirm that the method provides the highest ^{1}H resolution available today in ^{1}H MAS NMR of solids. We have also shown the application of this methodology to liquid-state data with a suitably adapted sequence.

Declaration of Competing Interest

The authors declare that they have no known competing financial interests or personal relationships that could have appeared to influence the work reported in this paper.

Acknowledgements

This work was supported by Swiss National Science Foundation Grant No. 200020_178860.

Appendix A. Supplementary material

Pulse sequences, processing codes, experimental parameters, measured linewidths and SNRs, and a link to the experimental NMR data.

Supplementary data to this article can be found online at https://doi.org/10.1016/j.jmr.2020.106856.

References

[1] M.M. Maricq, J.S. Waugh, J. Chem. Phys. 70 (1979) 3300–3316.
[2] a) E.R. Andrew, A. Bradbury, R.G. Eades, Nature 183 (1959) 1802–1803;
b) I.J. Lowe, Phys. Rev. Lett. 2 (1959) 285–287.
[3] a) V. Agarwal, S. Penzel, K. Szekely, R. Cadalbert, E. Testori, A. Oss, J. Past, A. Samoson, M. Ernst, A. Bockmann, B.H. Meier, Angew. Chem. Int. Ed. Engl. 53 (2014) 12253–12256;
b) T. Kobayashi, K. Mao, P. Paluch, A. Nowak-Krol, J. Sniechowska, Y. Nishiyama, D.T. Gryko, M.J. Potrzebowski, M. Pruski, Angew. Chem. Int. Ed. Engl. 52 (2013) 14108–14111;
c) Y.L. Lin, Y.S. Cheng, C.I. Ho, Z.H. Guo, S.J. Huang, M.L. Org, A. Oss, A. Samoson, J.C.C. Chan, Chem. Commun. (Camb.) 54 (2018) 10459–10462;
d) Y. Nishiyama, M. Malon, Y. Ishii, A. Ramamoorthy, J. Magn. Reson. 244 (2014) 1–5;
e) S. Penzel, A. Oss, M.L. Org, A. Samoson, A. Bockmann, M. Ernst, B.H. Meier, J. Biomol. NMR 73 (2019) 19–29.
[4] B.C. Gerstein, R.G. Pembleton, R.C. Wilson, L.M. Ryan, J. Chem. Phys. 66 (1977) 361–362.
[5] a) Z.H. Gan, P.K. Madhu, J.P. Amoureux, J. Trebosc, O. Lafon, Chem. Phys. Lett. 503 (2011) 167–170;
b) M.E. Halse, L. Emsley, J. Phys. Chem. A 117 (2013) 5280–5290;
c) M. Leskes, S. Steuernagel, D. Schneider, P.K. Madhu, S. Vega, Chem. Phys. Lett. 466 (2008) 95–99;
d) Y. Nishiyama, X. Lu, J. Trebosc, O. Lafon, Z. Gan, P.K. Madhu, J.P. Amoureux, J. Magn. Reson. 214 (2012) 151–158;
e) E. Salager, J.-N. Dumez, R.S. Stein, S. Steuernagel, A. Lesage, B. Elena-Herrmann, L. Emsley, Chem. Phys. Lett. 498 (2010) 214–220;
f) F.M. Paruzzo, L. Emsley, J. Magn. Reson. (2019) 309.
[6] P. Moutzouri, F.M. Paruzzo, B. Simões de Almeida, G. Stevanato, L. Emsley, Angew. Chem. Int. Ed. Engl. 59 (2020) 6235–6238.
[7] a) A.J. Pell, R.A. Edden, J. Keeler, Magn. Reson. Chem. 45 (2007) 296–316;
b) H. Oschkinat, A. Pastore, P. Pfandler, G. Bodenhausen, J. Magn. Reson. 69 (1986) 559–566.
[8] a) C.E. Avalos, B.J. Walder, J. Viger-Gravel, A. Magrez, L. Emsley, Phys. Chem. Chem. Phys. 21 (2019) 1100–1109;
b) M.C. Davis, K.M. Shookman, J.D. Sillaman, P.J. Grandinetti, J. Magn. Reson. 210 (2011) 51–58;
c) F.M. Paruzzo, B.J. Walder, L. Emsley, J. Magn. Reson. 305 (2019) 131–137;
d) B.J. Walder, K.K. Dey, D.C. Kaseman, J.H. Baltisberger, P.J. Grandinetti, J. Chem. Phys. 138 (2013) 174203.
[9] a) S.P. Brown, S. Wimperis, J. Magn. Reson. 128 (1997) 42–61;
b) S.P. Brown, S. Wimperis, J. Magn. Reson. 124 (1997) 279–285;
c) P.J. Grandinetti, J.H. Baltisberger, A. Llor, Y.K. Lee, U. Werner, M.A. Eastman, A. Pines, J. Magn. Reson. Ser. A 103 (1993) 72–81;
d) D. Massiot, B. Touzo, D. Trumeau, J.P. Coutures, J. Virlet, P. Florian, P.J. Grandinetti, Solid State Nucl. Magn. Reson. 6 (1996) 73–83.
[10] D. Massiot, J. Hiet, N. Pellerin, F. Fayon, M. Deschamps, S. Steuernagel, P.J. Grandinetti, J. Magn. Reson. 181 (2006) 310–315.
[11] L. Castanar, Magn. Reson. Chem. 55 (2017) 47–53.
[12] D.J. States, R.A. Haberkorn, D.J. Ruben, J. Magn. Reson. 48 (1982) 286–292.